

MIMO Predictive Control of a Wind Turbine

J. Novak, P. Chalupa

Abstract—In this work, linear model predictive control of a nonlinear wind-turbine model is studied. The wind turbine process is represented by a set of local linear models which are obtained by piecewise linearization of the nonlinear mathematical model at different wind speeds. In order to provide zero steady-state off-set in case of a disturbance or model/plant mismatch the model is augmented with disturbance model. Estimates of the states and wind are obtained with Extended Kalman Filter (EKF). The estimated wind is used for computation of weights of corresponding local models. Linear model parameters and estimated states are then used within predictive control strategy for computation of control signals. Due to different control demands in different operating regimes of the wind turbine the weighting matrices are also scheduled for different wind speeds. Simulations on the 5MW wind-turbine model in turbulent wind and comparison with baseline PI controller show that the wind-turbine system can be successfully controlled at different operating regions by this methodology.

Keywords—Extended Kalman filter, Multiple model, Predictive control, Wind turbine.

I. INTRODUCTION

TODAY, wind power accounts for the largest share of renewable energy generation after hydropower, with 30% global annual growth. In 2012, the European Union installed capacity of wind turbines reached 105 000MW. The energy available in the wind is obtained through the wind conversion process, which is strongly nonlinear and challenging from the control system viewpoint as the power obtained from the wind is proportional to the third power of the effective wind speed. The wind turbines are operated in strong noisy environments and with severe constraints on admissible loads. The control problems are even more challenging when turbines are able to operate at variable speed and variable pitch. The best use of this type of turbine can only be achieved by means of multivariable controllers. The effective control strategy also reduces structural fatigue and load on the drive-train and tower structure, leading to potentially longer lifetime of the wind turbine [1].

Advanced control methods for addressing these issues have been investigated for two decades but apparently most commercial systems are still implemented using multiple

single-input-single-output (SISO) control loops [2],[3]. Conventional PI controllers have been tested in [3]. In [1] gain scheduling control is addressed in the context of linear parameter varying systems. The multivariable controller design is stated as an optimization problem with linear matrix inequalities. Barambones et al. proposed sliding mode control law for variable speed wind turbine in [4].

The neural network controller is developed for control of pitch angle of wind turbines rotor blades in [5]. Soliman et al. developed a Multiple Model Predictive controller to control variable speed variable-pitch wind turbine over its full operating range [6]. Robust control techniques of the same type of wind turbine have been investigated in [7], [8]. To cope with nonlinear behavior of the system, adaptive control approaches have been proposed in [9], [10], [11], [12]. The fuzzy logic controller was applied in [13] to control a small size wind energy conversion system. In [14] the control scheme that consists of inner loop for generator torque regulation using a fuzzy control and outer loop for pitch control based on least square support vector machine is developed. In order to reduce the life-time fatigue and reduce the load in extreme gusts nonlinear predictive controller and LIDAR (Light Detection and Ranging) system for prediction of future wind is tested in [15].

This work presents application of the multi-input multi-output (MIMO) predictive control with constraints on the model of the 5MW wind turbine. In Section 2, nonlinear mathematical model of the wind turbine with the augmented wind model is addressed and the linearization of this model for different wind speeds is given. The operating regions and different control strategies in these regions are presented in Section 3. Section 4 describes the process of estimation of the states and immeasurable disturbances using multiple Extended Kalman Filters. The concept of predictive control with multiple linear models and constraints is introduced in Section 5. Finally, in Section 6, simulation results for model of the 5MW wind turbine in turbulent wind conditions are shown with brief conclusion.

II. MATHEMATICAL MODEL OF A WIND TURBINE

Today the most wide spread version of wind energy conversion system (WECS) is the horizontal axis wind turbine (HAWT) with a 3 blade upwind rotor (Fig. 1) due to its higher efficiency and lower cost-to-power ratio. The WECS can work by fixed and variable speed. Variable-speed generation is claimed to have a better energy capture and lower loading. In this section the first principle model of variable-speed variable-pitch HAWT is addressed.

Jakub Novak is with Faculty of Applied Informatics, Tomas Bata University in Zlin, nam. T.G. Masaryka 5555, 76001 Zlin, Czech Republic (email: jnovak@fai.utb.cz)

Petr Chalupa is with Faculty of Applied Informatics Tomas Bata University in Zlin, nam. T.G. Masaryka 5555, 76001 Zlin, Czech Republic (email: chalupa@fai.utb.cz).

The research was supported by the European Regional Development Fund under the project CEBIA-Tech No. CZ.1.05/2.1.00/03.0089. This assistance is very gratefully acknowledged.

The wind turbine characteristics can be divided into 4 parts:

- Aerodynamics
- Turbine mechanics
- Generator dynamics
- Actuator dynamics

The available power of the wind in a circular cross section with the same area as the rotor disc is given by [16] :

$$P_w = \frac{1}{2} \rho \pi R_m^2 v^3 \quad (1)$$

where ρ is the air density (1.2 kg/m^3), R_m is the blade radius and v is the effective wind speed. Only a fraction of the available power P_w is can be converted to the rotor power P_r . This ration is given by coefficient c_p

$$P_r = P_w c_p \quad (2)$$

Power coefficient c_p have a theoretical upper limit of 0.593 known as the Betz limit. The rotor blades convert the kinetic energy of the wind into mechanical energy, providing the torque T_r on the rotor:

$$T_r = \frac{P_r}{\omega_r} \quad (3)$$

where the ω_r is the rotational speed. The power coefficient c_p is a function of tip speed ratio λ and blade pitch angle θ . The tip speed ratio λ is given as a ratio between effective wind velocity and the blade tip speed:

$$\lambda = \frac{v}{R_m \omega_r} \quad (4)$$

The values of power coefficient are usually provided in the form of look-up table [17]. A three dimensional plot of efficiency coefficient c_p is depicted on Fig. 2 and corresponding power curves for $\theta = 0, 5, 10, 20$ degrees are shown in Fig. 3.

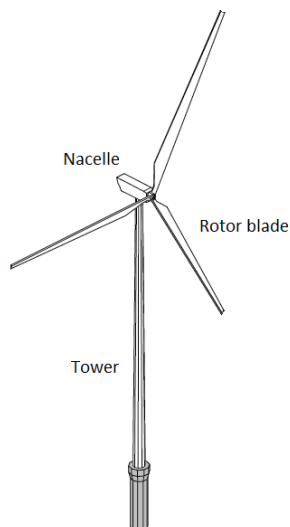


Fig. 1 Horizontal axis wind turbine

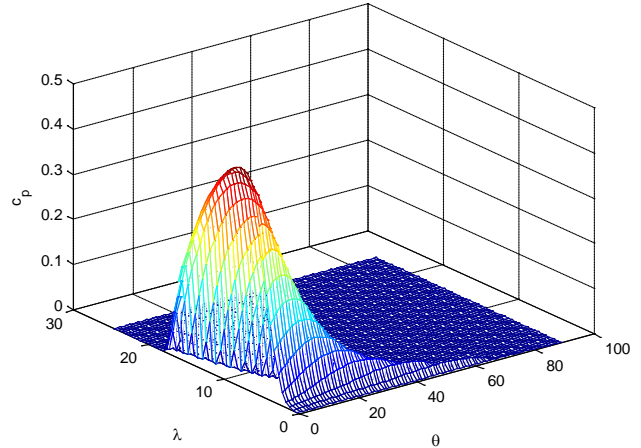


Fig. 2 The efficiency coefficient c_p as a function of tip speed ratio and blade pitch angle (negative values were zeroed)

As can be seen the power coefficient changes with tip-speed ratio variations for a specified pitch angle, and there is a single value of λ for which the corresponding c_p is maximized.

The generated power P_e is given by:

$$P_e = T_g \omega_g \quad (5)$$

where ω_g is rotational speed of the generator.

The generator torque can be manipulated and is approximated by a first order system with time constant τ_T :

$$\dot{T}_g = -\frac{1}{\tau_T} T_g + \frac{1}{\tau_T} T_{gr} \quad (6)$$

where T_{gr} is the reference value for actuator's output. The pitch of the blades is also changed by actuator with first order dynamics with time constant τ_θ :

$$\dot{\theta} = -\frac{1}{\tau_\theta} \theta + \frac{1}{\tau_\theta} \theta_r \quad (7)$$

where θ_r is the blade pitch angle reference value.

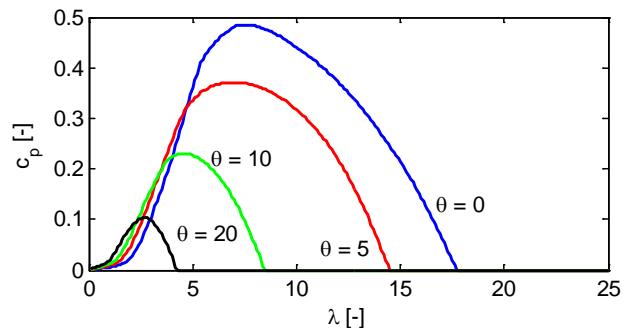


Fig. 3 Power curves

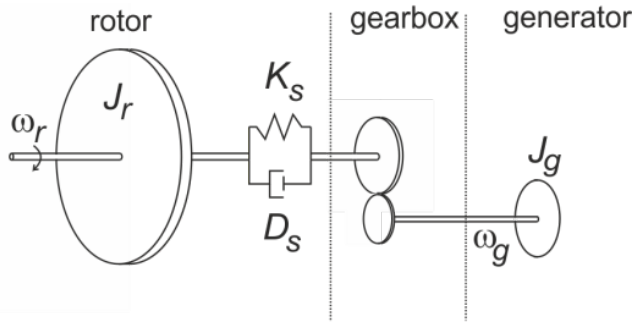


Fig. 4 Schematic of the wind turbine mechanics

The mechanistic part of the turbine (as depicted on Fig. 4) can be divided into rotor and generator side connected by a shaft. The dynamic nature of the shaft is described by the damping D_s and spring constant K_s . The torques acting on each side of the transmission are related by the gear ratio N_g . The gearbox is used to step up the low angular speeds of the turbine to the high rotational speeds of the generator.

Using the Newton's second law for rotating bodies the following equations can be formulated to describe the dynamics of the mechanical part of the wind turbine:

$$\dot{\omega}_r = \frac{P_r}{\omega_r J_r} - \frac{\omega_r D_s}{J_r} + \frac{\omega_g D_s}{J_r N_g} - \frac{\delta K_s}{J_r} \quad (8)$$

$$\dot{\omega}_g = \frac{\omega_r D_s}{N_g J_g} - \frac{\omega_g D_s}{N_g^2 J_g} + \frac{\delta K_s}{J_g N_g} - \frac{T_g}{J_g} \quad (9)$$

$$\dot{\delta} = \omega_r - \frac{\omega_g}{N_g} \quad (10)$$

where variable δ describes the twist of the shaft, J_r and J_g are the rotor and generator inertia, respectively. The moments of inertia of the shafts and gearbox are neglected because they are small compared with moment of inertia of the rotor and generator.

The energy available in the wind varies as the cube of the wind speed, so the characteristic of the wind resource is critical to all wind turbine control strategies. In the paper the effective wind velocity is modeled as a mean wind velocity v_m superimposed by turbulent wind velocity v_t to simulate the temporal variations of the wind:

$$v = v_m + v_t \quad (11)$$

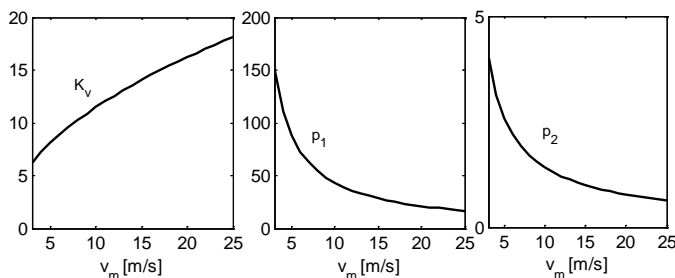


Fig. 5 Filter parameters for different wind speed

The turbulent part of the wind velocity is modeled as a second order filter driven by a white noise process [18]:

$$v(t) = \frac{K_v}{(p_1 s + 1)(p_2 s + 1)} e(t) \quad (12)$$

where $e(t)$ is a white noise with unity variance. The parameters p_1, p_2, K_v are found by second order approximation of the wind power spectrum density dominant in unstable wind conditions [19]:

$$Sp(f) \frac{f}{v_r^2} = \frac{105 \frac{f}{1+15 \frac{h}{h_i}}}{\left(1+33 \frac{f}{1+15 \frac{h}{h_i}}\right)^{\frac{5}{3}} \left(1+15 \frac{h}{h_i}\right)^{\frac{2}{3}}} \quad (13)$$

where f is the frequency, h is the nacelle height and h_i is the height of the lowest inversion. Dependency of the parameters p_1, p_2, K_v on the mean wind speed is presented on Fig. 5.

The equivalent state-space formulation of the wind speed model is:

$$\dot{v}_t = \dot{v}_t \quad (14)$$

$$\dot{v}_t = -\frac{1}{p_1 p_2} v_t - \frac{p_1 + p_2}{p_1 p_2} \dot{v}_t + \frac{K_v}{(p_1 p_2)} e \quad (15)$$

Equations (5)-(12) are combined to yield the nonlinear model of the wind turbine:

$$\begin{bmatrix} \dot{\omega}_r \\ \dot{\omega}_g \\ \dot{\delta} \\ \dot{\theta} \\ \dot{T}_g \\ \dot{v}_t \\ \dot{\dot{v}}_t \end{bmatrix} = \begin{bmatrix} \frac{P_r(\omega_r, \theta, v_m + v_t)}{\omega_r J_r} - \frac{\omega_r D_s}{J_r} + \frac{\omega_g D_s}{J_r N_g} - \frac{\delta K_s}{J_r} \\ \frac{\omega_r D_s}{N_g J_g} - \frac{\omega_g D_s}{N_g^2 J_g} + \frac{\delta K_s}{J_g N_g} - \frac{T_g}{J_g} \\ \omega_r - \frac{\omega_g}{N_g} \\ -\frac{1}{\tau_\theta} \theta \\ -\frac{1}{\tau_T} T_g \\ \dot{v}_t \\ -\frac{1}{p_1 p_2} v_t - \frac{p_1 + p_2}{p_1 p_2} \dot{v}_t \end{bmatrix} + \begin{bmatrix} 0 \\ 0 \\ 0 \\ \frac{1}{\tau_\theta} \\ 0 \\ 0 \\ 0 \end{bmatrix} \begin{bmatrix} \theta_r \\ T_{gr} \end{bmatrix} + \begin{bmatrix} 0 \\ 0 \\ 0 \\ 0 \\ 0 \\ 0 \\ \frac{K_v}{(p_1 p_2)} \end{bmatrix} e \quad (16)$$

The slow varying element of the wind velocity v_m is assumed to be known. The fuzzy global model of the process is obtained through piecewise linearization.

The nonlinear system:

$$\dot{x}(t) = f(x(t), u(t)) \quad (17)$$

$$y(t) = g(x(t), u(t)) \quad (18)$$

where $x(t) \in R^n, u(t) = R^p, y(t) = R^q$ represent the states, input and output, respectively. The system is linearized around the operating point using the Taylor's series approximation. This results in a series of M local linear models of the form:

$$\begin{aligned} \delta \dot{x}_i(t) &= \mathbf{A}_i \delta x(t) + \mathbf{B}_i \delta u(t) \\ \delta y_i(t) &= \mathbf{C}_i \delta x(t) + \mathbf{D}_i \delta u(t) \end{aligned} \quad (19)$$

where

$$\begin{aligned} \mathbf{A}_i &= \frac{\partial f(x, u)}{\partial x} \Big|_{(x^{opi}, u^{opi})} \\ \mathbf{B}_i &= \frac{\partial f(x, u)}{\partial u} \Big|_{(x^{opi}, u^{opi})} \\ \mathbf{C}_i &= \frac{\partial g(x, u)}{\partial x} \Big|_{(x^{opi}, u^{opi})} \\ \mathbf{D}_i &= \frac{\partial g(x, u)}{\partial u} \Big|_{(x^{opi}, u^{opi})} \\ \delta x_i &= x_i - x_i^{opi}, \delta u_i = u_i - u_i^{opi}, \\ \delta y_i &= y_i - y_i^{opi} \end{aligned} \quad (20)$$

As the controller will be working in all operating modes it is beneficial to convert the incremental model into affine and discretize to yield model in the form:

$$\mathbf{x}_i(k+1) = \mathbf{A}_i \mathbf{x}_i(k) + \mathbf{B}_i \mathbf{u}_i(k) + \mathbf{E}_i \quad (21)$$

$$\mathbf{y}_i = \mathbf{C}_i \mathbf{x}_i(k) + \mathbf{F}_i \quad (22)$$

The model is assumed not to have direct feed through so $D = 0$. In order to provide off-set free control in case of unmeasured disturbances and modeling errors the model is augmented with the model of unmeasured input disturbances with integral character [19]:

$$d(k+1) = d(k) + e(k) \quad (23)$$

$$p(k+1) = p(k) + e(k) \quad (24)$$

The augmented system is then given as:

$$\begin{bmatrix} \mathbf{x}(k+1) \\ d(k+1) \\ p(k+1) \end{bmatrix} = \begin{bmatrix} \mathbf{A}_i & \mathbf{B}_i \\ 0 & 1 & 0 \\ 0 & 0 & 1 \end{bmatrix} \begin{bmatrix} \mathbf{x}(k) \\ d(k) \\ p(k) \end{bmatrix} + \begin{bmatrix} \mathbf{B}_i \\ 0 \\ 0 \end{bmatrix} \mathbf{u}(k) + \begin{bmatrix} \mathbf{E}_i \\ e(k) \\ e(k) \end{bmatrix} \quad (25)$$

$$\mathbf{y}(k) = [\mathbf{C}_i \quad 0 \quad 0] \begin{bmatrix} \mathbf{x}(k) \\ d(k) \\ p(k) \end{bmatrix} + \mathbf{F}_i \quad (26)$$

The augmented model is used for state estimation in extended Kalman filter.

III. OPERATING MODES OF THE WIND TURBINE

The objective for controlling a wind turbine is to maximize power production and minimize mechanical stress on the components of the wind turbine. The wind turbine can be operated in four different regimes (Fig. 6) depending on the wind speed. If the wind is too low to warrant turbine startup the blades are pitch to angle that generates minimum aerodynamic torque. In the region I where the wind speed large enough for machine start-up the rotational speed of the rotor ω_r is kept at its lowest allowable level. The control strategy is to keep the pitch of the blades at the optimum value and control the system by manipulating the generator torque T_g . In the region II the rotational speed of the rotor ω_r is within the limits $\omega_{r,min} < \omega_r < \omega_{r,max}$ and the blade pitch is kept at the optimum value providing the maximization of c_p and aerodynamic torque. The maximal value of c_p is for blade pitch $\theta = 0$ and tip speed ratio $\lambda = 7.5$. Each wind speed has corresponding rotor speed that generates greatest possible aerodynamic torque.

The primary objective is to keep tip speed ratio at its optimal value $\omega_{opt} = \frac{Rm\lambda_{opt}}{v}$ to maximize turbine's aerodynamic efficiency. In the region III the rotational speed of the rotor ω_r is at its maximum but generated power P_e is below its nominal value. In this transition region is system is controlled the same way as in the region II. In the top region IV both the rotational speed of the rotor ω_r and generated power P_e are at their rated values. In this region the torque is kept constant and blade pitch θ is used to compensate the variation in wind power.

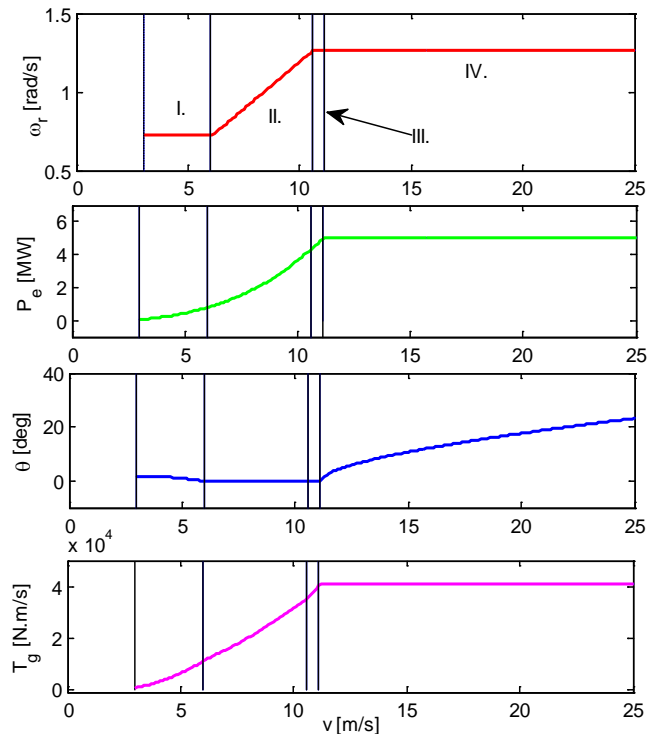


Fig. 6 Operation modes of the NREL wind turbine

IV. STATE ESTIMATION WITH EXTENDED KALMAN FILTER

Not all the states of the variable speed wind turbine system can be measured and furthermore the measurement of available outputs is bound to be corrupted with measurement noise. In order to estimate the states of the nonlinear model the extended Kalman Filter (KF) is designed. The extended KF is the nonlinear extension of the linear Kalman filter where the model is nonlinear [20]:

$$x(k+1) = f(x(k), u(k)) + w \quad (27)$$

$$y(k) = g(x(k)) + v \quad (28)$$

where w and v are process and measurement noises, which are assumed to have Gaussian distribution with covariances \mathbf{Q}_k and \mathbf{R}_k . Since the system is nonlinear the Jacobians are used instead of nonlinear expressions to compute covariance and consequently Kalman gain. The update equations of the EKF are given as:

$$\hat{x}(k+1|k) = f(\hat{x}(k|k), \mathbf{u}(k)) + \mathbf{K}(k)[\mathbf{h}(k) - g(\hat{x}(k|k))] \quad (29)$$

$$\mathbf{K}(k) = \frac{\mathbf{P}\mathbf{H}^T(k)}{\mathbf{H}(k)\mathbf{P}\mathbf{H}^T(k) + \mathbf{R}_k} \quad (30)$$

where \mathbf{P} is the estimation covariance error matrix, $\mathbf{h}(k)$ is the measured output vector, $\mathbf{K}(k)$ is the Kalman gain. The covariance error matrix is obtained as a solution of algebraic Riccati equation:

$$\mathbf{P} = \mathbf{Q}_k + \mathbf{F}(k)\mathbf{P}\mathbf{F}^T(k) - \frac{(\mathbf{F}^T(k)\mathbf{H}(k))(\mathbf{F}^T(k)\mathbf{H}(k))^T}{(\mathbf{H}^T(k)\mathbf{H}(k) + \mathbf{R}_k)} \quad (31)$$

The linearization of the functions $f(x, u), g(x)$ is accomplished off-line during the modeling process and the Jacobians can be computed using the linearized local models matrices as:

$$\mathbf{F}(k) = \left. \frac{\delta f}{\delta x} \right|_{x(k)=\hat{x}(k|k)} = \mathbf{A}_i \quad (32)$$

$$\mathbf{H}(k) = \left. \frac{\delta g}{\delta x} \right|_{x(k)=\hat{x}(k|k)} = \mathbf{C}_i \quad (33)$$

V. MODEL-BASED PREDICTIVE CONTROL

In this chapter the concept of model predictive control (MPC) is presented. Model-based predictive control (MPC) has been successfully used in many industrial applications due to its ability to handle MIMO control problems with constraints on the system variables [21]. The objective for control of a wind turbine is to maximize power production and minimize the mechanical stress on the components of the wind turbine. In order to control the wind turbine in the whole spectrum of wind speeds the parameters of model are scheduled based on the current mean wind speed. The state-space model based predictive control is based on linear time varying model that is obtained at every sampling interval and

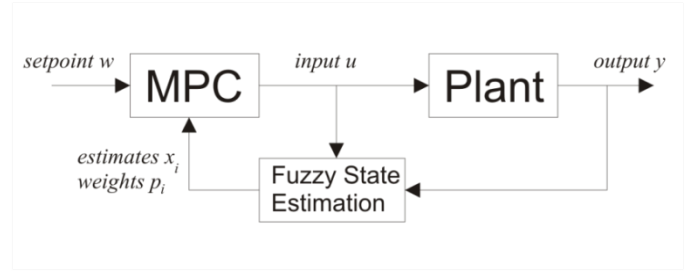


Fig. 7 Multiple model predictive control scheme

its parameters are used for the entire prediction horizon H_p :

$$x(k+1) = \mathbf{A}x(k) + \mathbf{B}u(k) + \mathbf{E}$$

$$y(k) = \mathbf{C}x(k) + \mathbf{F}$$

$$\mathbf{A} = \sum_{i=1}^M p_i \mathbf{A}_i, \mathbf{B} = \sum_{i=1}^M p_i \mathbf{B}_i, \mathbf{E} = \sum_{i=1}^M p_i \mathbf{E}_i \quad (34)$$

$$\mathbf{C} = \sum_{i=1}^M p_i \mathbf{C}_i, \mathbf{F} = \sum_{i=1}^M p_i \mathbf{F}_i$$

where p_i are the weights of each local model and are a function of the current wind speed [22]. The control structure for the model predictive control with multiple local models is shown in the block diagram in Fig. 7.

The computation of a control law of MPC is based on minimization of the following criterion:

$$J_{MPC} = (\hat{\mathbf{Y}} - \mathbf{W})^T \mathbf{Q}(\hat{\mathbf{Y}} - \mathbf{W}) + \Delta \mathbf{U} \mathbf{R} \Delta \mathbf{U} + (\mathbf{U} - \mathbf{U}_s) \mathbf{S} (\mathbf{U} - \mathbf{U}_s) \quad (35)$$

with input constraints:

$$u_{min} \leq u(k+j) \leq u_{max} \quad (36)$$

$$\Delta u_{min} \leq \Delta u(k+j) \leq \Delta u_{max} \quad (37)$$

where $j = 1, 2, \dots, H_c - 1$, H_c is the control horizon, $\hat{\mathbf{Y}}$ is a vector future prediction of the system, \mathbf{W} is a vector of reference trajectory and $\mathbf{Q}, \mathbf{R}, \mathbf{S}$ are positive definite weighting matrices. The last term $(\mathbf{U} - \mathbf{U}_s)$ represents the deviation from inputs that led to linearization point of the model. The predictor $\hat{\mathbf{Y}} = [y(k) \dots y(k+N_p)]^T$ for any given prediction and control horizons for control sequence $\mathbf{U} = [u(k) \dots u(k+N_c-1)]^T$ can be computed using the iterative algorithm:

$$\hat{\mathbf{Y}} = \Phi_x x(k) + \begin{bmatrix} \Phi_1 \\ \Phi_2 \end{bmatrix} \mathbf{U} + \Phi_0 \quad (38)$$

with

$$\Phi_x = \begin{bmatrix} \mathbf{C}\mathbf{A} \\ \mathbf{C}\mathbf{A}^2 \\ \vdots \\ \mathbf{C}\mathbf{A}^{N_p-1} \end{bmatrix}, \Phi_0 = \begin{bmatrix} \mathbf{C}\mathbf{E} + \mathbf{F} \\ \mathbf{C}\mathbf{A}\mathbf{E} + \mathbf{C}\mathbf{E} + \mathbf{F} \\ \vdots \\ \mathbf{C}\mathbf{A}^{N_p-1}\mathbf{E} + \dots + \mathbf{C}\mathbf{E} + \mathbf{F} \end{bmatrix} \quad (39)$$

and

$$\Phi_1 = \begin{bmatrix} CB & 0 & \dots & 0 \\ CAB & CB & \dots & 0 \\ \vdots & \vdots & \ddots & 0 \\ CA^{N_c-1}B & CA^{N_c-2}B & \dots & CB \end{bmatrix} \quad (40)$$

$$\Phi_2 = \begin{bmatrix} CA^{N_c}B & \dots & CA^2B & CB \sum_{j=0}^1 A^j \\ \vdots & \vdots & \vdots & \vdots \\ CA^{N_p-1}B & \dots & CA^{N_p-N_c+1}B & CB \sum_{j=0}^{N_p-N_c} A^j \end{bmatrix} \quad (41)$$

The minimization of the cost criterion (35) can be transformed into a quadratic programming problem:

$$J_{MPC} = \mathbf{u}^T \mathbf{H} \mathbf{u} + \mathbf{f} \mathbf{u} \quad (42)$$

with constraints:

$$\mathbf{A} \mathbf{u} \leq \mathbf{b} \quad (43)$$

and solved numerically at each sampling instant.

VI. IMPLEMENTATION

The wind turbine that is being considered in the paper is a wind turbine model widely known as ‘‘NREL offshore 5-MW baseline wind turbine’’ that was developed by ‘‘National Renewable Energy Laboratory’’ of the United States of America. This wind turbine is a conventional three-bladed upwind variable-speed variable blade-pitch-to-feather-controlled turbine. The parameters of the model are presented in Table I [23].

Table I NREL wind turbine parameters

parameter	units	value
nominal power $P_{e,norm}$	[MW]	5
rated rotor speed $\omega_{r,max}$	[rad/s]	1.2671
drive-train spring const. K_s	[N.m/rad]	867.637E6
drive-train damp. const. D_s	[N.m/rad.s]	6.215E6
generator inertia J_g	[kg.m ²]	534.116
rotor inertia J_r	[kg.m ²]	3.8768E7
blade radius R_m	[m]	63
gear ratio N_g	[-]	97
max blade pitch θ_{max}	[deg]	90
min blade pitch θ_{min}	[deg]	0
max bl. pitch rate $\Delta\theta_{max}$	[deg/s]	8
min bl. pitch rate $\Delta\theta_{min}$	[deg/s]	-8
max gen. torque $T_{g,max}$	[N.m]	47402.97
min gen. torque $T_{g,min}$	[N.m]	0
max gen. torque rate $\Delta T_{g,max}$	[N.m/s]	15000
min gen. torque rate $\Delta T_{g,min}$	[N.m/s]	-15000
pitch actuator const. τ_θ	[s]	0.12
gen. actuator const. τ_T	[s]	0.1

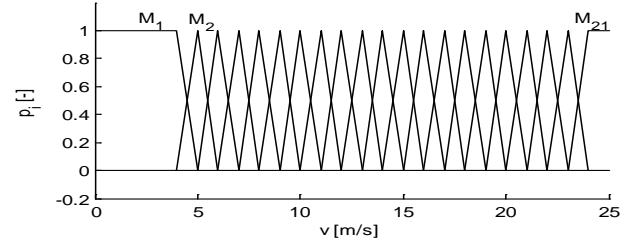


Fig. 8 Fuzzy membership functions

Seventh order nonlinear model (16) was implemented in MATLAB with multiple Kalman filters and MPC controller. The controller is compared with the baseline controller developed in [23] that uses two independent control loops for torque and blade pitch angle control and measurement filter. The control of the torque is proportional to the filtered generator speed and the control of blade pitch angle is based on the gain scheduled PI controller. In the proposed control scheme the wind turbine is controlled in all regions. As the dynamics of the system is different for different wind speeds a local model was obtained by linearization of the nonlinear model of the process. 21 local models were developed for mean wind speed $v \in (4,25)$. The parameters of the system between these local models are obtained using fuzzy membership function as shown on Fig. 8. The sampling period T_s is chosen to be 0.025s. It is assumed that only the generator speed ω_g , blade pitch θ and output power P_e can be measured and the mean wind speed v_m is assumed to be known:

$$h(k) = \begin{bmatrix} x_2 \\ x_4 \\ x_2 x_5 \end{bmatrix} = \begin{bmatrix} \omega_g \\ \theta \\ P_e \end{bmatrix} \quad (44)$$

The other system states and unmeasured disturbances are estimated via extended Kalman filter. Due to imperfection of the measurement device the measurement noise is added to the output of the wind turbine model:

$$h(k) = \begin{bmatrix} \omega_g \\ \theta \\ P_e \end{bmatrix} + 0.03 \begin{bmatrix} \omega_g e(k) \\ \theta e(k) \\ P_e e(k) \end{bmatrix} \quad (45)$$

where $e(k)$ is a Gaussian white noise. All the states of the augmented model are observable as the row rank of the observability matrix equals the number of states:

$$\text{rank} \begin{bmatrix} C \\ CA \\ \vdots \\ CA^8 \end{bmatrix} = 9 \quad (46)$$

Since the wind does not affect the actuators' states the process noise is added to these states in order to obtain nonzero Kalman gain. The process noise covariance matrix is then given as:

$$Q_k = [B \quad B_v \quad B_{pd}] M \begin{bmatrix} B^T \\ B_v^T \\ B_{pd}^T \end{bmatrix} \quad (47)$$

$$M = \begin{bmatrix} 0.001 & 0 & 0 & 0 & 0 \\ 0 & 0.1 & 0 & 0 & 0 \\ 0 & 0 & 1 & 0 & 0 \\ 0 & 0 & 0 & 0.001 & 0 \\ 0 & 0 & 0 & 0 & 0.1 \end{bmatrix} \quad (48)$$

$$B = \begin{bmatrix} 0 & 0 \\ 0 & 0 \\ 0 & 0 \\ \frac{T_s}{\tau_\theta} & 0 \\ 0 & \frac{T_s}{\tau_T} \\ 0 & 0 \\ 0 & 0 \\ 0 & 0 \\ 0 & 0 \end{bmatrix} B_{pd} = \begin{bmatrix} 0 & 0 \\ 0 & 0 \\ 0 & 0 \\ 0 & 0 \\ 0 & 0 \\ \frac{T_s}{\tau_\theta} & 0 \\ \tau_\theta & \frac{T_s}{\tau_T} \\ 0 & \tau_T \end{bmatrix} \quad (49)$$

$$B_v = \left[0 \ 0 \ 0 \ 0 \ 0 \ 0 \ \frac{K_v T_s}{p_1 p_2} \ 0 \ 0 \right]^T \quad (50)$$

The measurement covariance matrix was set to [24]:

$$R_k = \frac{2}{500} \begin{bmatrix} \left(\frac{0.03\theta}{3}\right)^2 & 0 & 0 \\ 0 & \left(\frac{0.03\omega_g}{3}\right)^2 & 0 \\ 0 & 0 & \left(\frac{0.03P_e}{3}\right)^2 \end{bmatrix} \quad (51)$$

Model predictive controller was employed for computation of manipulated variables. Prediction and control horizons were set to:

$$H_p = 2s, H_c = 1s \quad (52)$$

For such values acceptable performance was obtained and these values does not represent big computational burden for the processing unit. The MPC was implemented with constraint on the blade pitch and generator torque given by:

$$\theta_{min} \leq \theta \leq \theta_{max} \quad (53)$$

$$T_{g,min} \leq T_g \leq T_{g,max} \quad (54)$$

$$\Delta\theta_{min} \leq \Delta\theta \leq \Delta\theta_{max} \quad (55)$$

$$\Delta T_{g,min} \leq \Delta T_g \leq \Delta T_{g,max} \quad (56)$$

The weights for the MPC were also scheduled using fuzzy membership function and their values for different wind speeds are presented in Table II.

Table II MPC weights scheduling

v	4-10 m/s	11m/s	12-25 m/s
Q	$\begin{bmatrix} 10^2 & 0 \\ 0 & 10^{-10} \end{bmatrix}$	$\begin{bmatrix} 10^2 & 0 \\ 0 & 10^{-10} \end{bmatrix}$	$\begin{bmatrix} 10^1 & 0 \\ 0 & 10^{-10} \end{bmatrix}$
R	$\begin{bmatrix} 10^6 & 0 \\ 0 & 10^{-2} \end{bmatrix}$	$\begin{bmatrix} 10^4 & 0 \\ 0 & 10^{-3} \end{bmatrix}$	$\begin{bmatrix} 10^3 & 0 \\ 0 & 10^{-3} \end{bmatrix}$
S	$\begin{bmatrix} 10^5 & 0 \\ 0 & 0 \end{bmatrix}$	$\begin{bmatrix} 10^1 & 0 \\ 0 & 0 \end{bmatrix}$	$\begin{bmatrix} 0 & 0 \\ 0 & 0 \end{bmatrix}$

The acceptable performance is obtained with Kalman filter estimation scheme. The measured outputs affected by the noise are presented in Fig. 9. Only 5s of the experiment is shown for clarity. To illustrate the precision of the estimates, the state estimation errors $\Delta x = x - \hat{x}$ are also presented in Fig. 10.

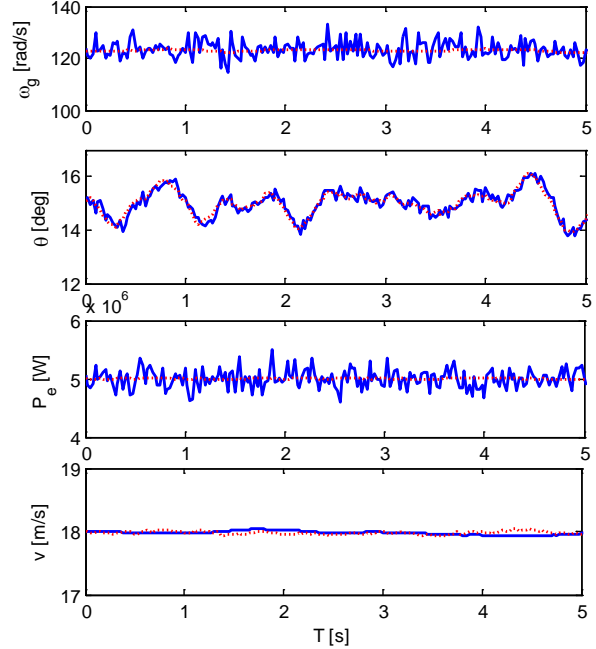


Fig. 9 Estimation of the states (blue solid – measured outputs, red dotted - estimates)

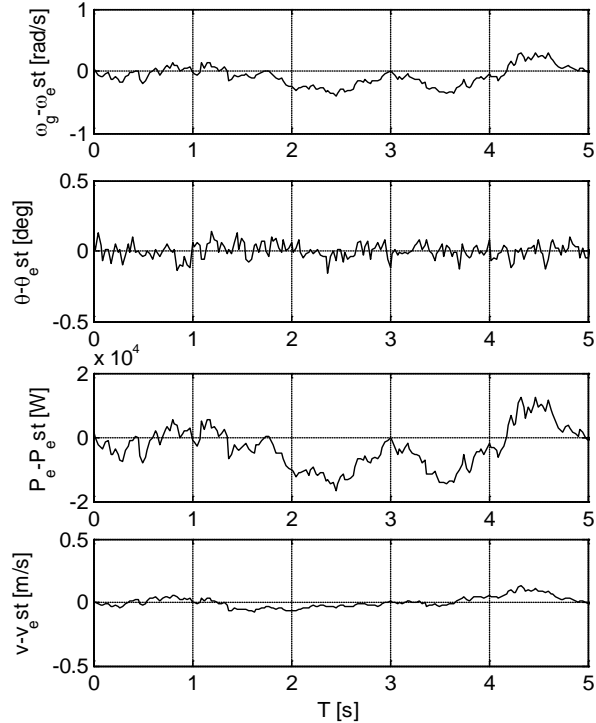


Fig. 10 Estimation errors from true states

The performance of the proposed predictive control was compared with baseline controller. The whole 10 min simulation with predictive controller with stochastic wind

disturbance (Fig. 11) is presented in Figs. 12, 13 and 14. The same wind sequence was used for both controllers. The control performance in terms of mean values, standard deviations and sum of control increments are also shown in Table III in order to prove the improved performance. Table shows the 50% decrease of standard deviation of output power and also decrease of oscillation of the control torque and thus reduction of load. The MPC strategy does not have significant impact on the mean values of controlled signals.

Table III Control performance comparison

	PI control	MPC
Mean ω_g	122,9083	122,9091
Mean P_e	5,000E6	5,000E6
Std ω_g	0,43	0,39
Std P_e	5,03E3	2,07E3
$\sum \Delta\theta$	0,0434	0,027
$\sum \Delta T_g$	4,49E4	2,49E4

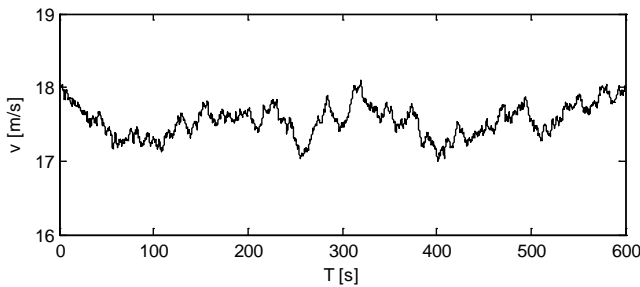


Fig. 11 Stochastic wind disturbance

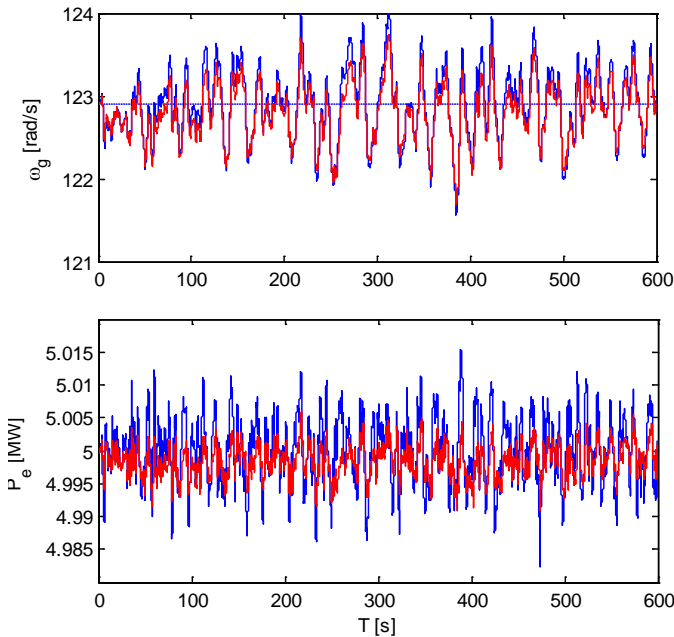


Fig. 12 Performance evaluation – output values (blue – baseline PI controller, red– MPC)

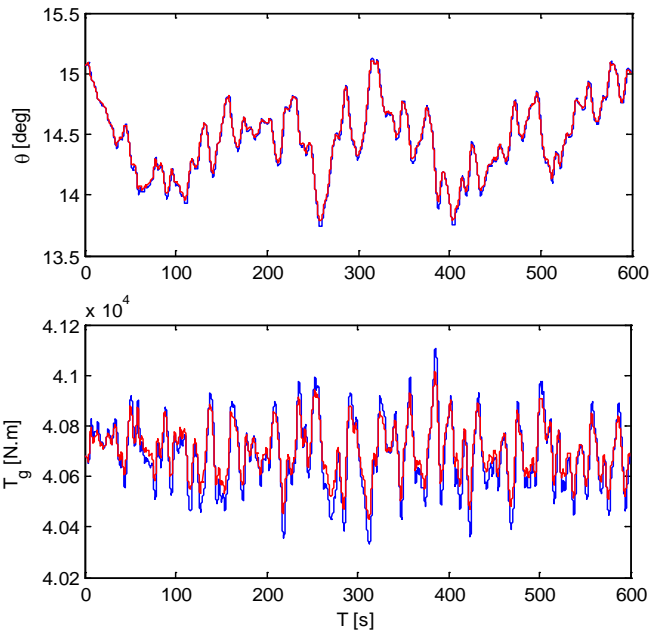


Fig. 13 Performance evaluation – pitch angle and generator torque (blue – baseline PI controller, red – MPC)

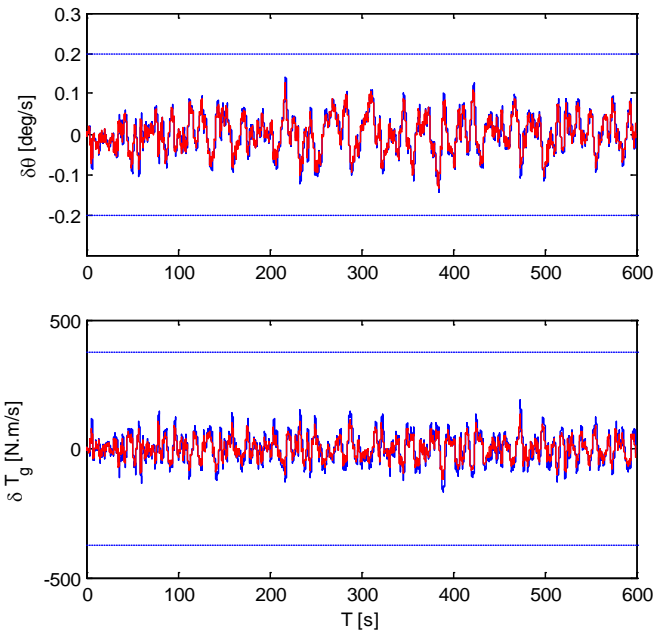


Fig. 14 Performance evaluation – pitch angle and generator torque speed of change (blue – baseline PI controller, red– MPC)

The proposed control strategy was also tested through simulation with turbulent wind that drives the turbine through different operating modes. With the MPC weights given in the Table II both the output power and rotor speed are tracked accurately in region IV. For low wind speeds optimal tip speed ratio is the main aim of control.

The turbulent wind affecting the wind turbine during the simulation is presented in Fig. 15. The control courses for reference tracking test are presented in Fig. 16 and 17. In the region II the main focus of the control is to maximize the

power so the power coefficient plot during the experiment is also presented in Fig. 18.

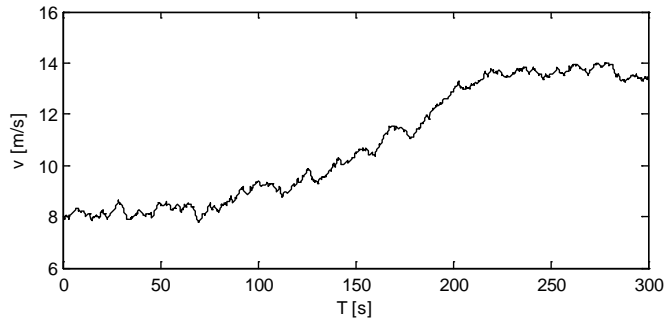


Fig. 15 Turbulent wind in the simulation

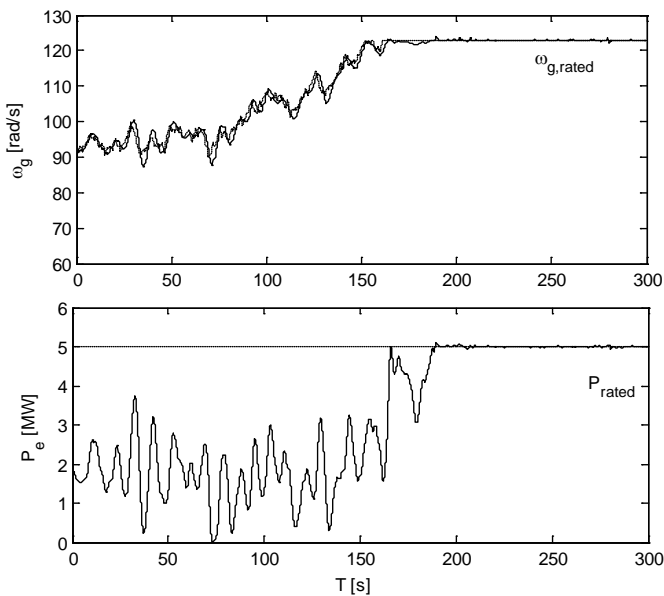


Fig. 16 Wind turbine's power output P_e and generator speed ω_g in simulation with turbulent wind

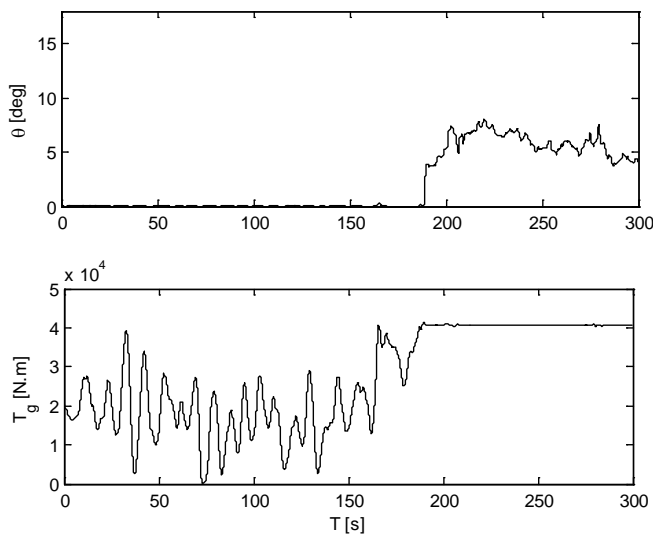


Fig. 17 Blade pitch angle θ and generator torque T_g in simulation with turbulent wind

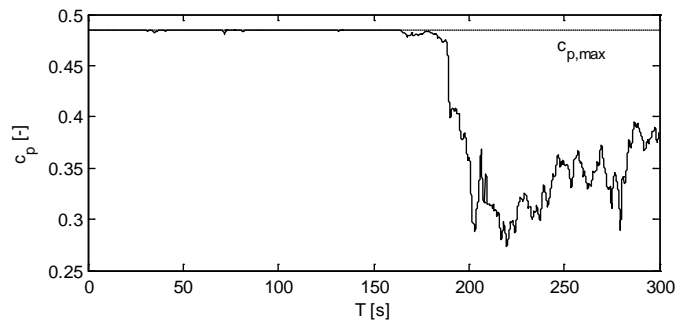


Fig. 18 Tip speed ratio in simulation with turbulent wind

In the region II the large variation of the electric power P_e can be observed. This is due to the fact that the main focus is put on tracking of the rotor rotational speed ω_r and consequently optimal tip speed ratio λ . In this region the produced power P_e is closely linked with the generator torque T_g .

VII. CONCLUSION

In the paper, fuzzy predictive control concept is applied to the model of 5MW wind turbine. It was assumed that measurement noise was present and not all the states are measurable to make the control more realistic. The weight scheduled predictive controller was implemented for control of the wind turbine in all operating regimes in a smooth way under the turbulent wind conditions. It has been shown that significant improvements in terms of control performance can be obtained with MPC strategy.

REFERENCES

- [1] F.D. Bianchi, H. Batista, R.J. Mantz, *Wind Turbine Control Systems: Principles, Modelling and Gain Scheduling Design*. New York: Springer-Verlag, 2007.
- [2] J.H. Laks, L.Y. Pao, A. D. Wright, "Control of Wind Turbines: Past, Present, and Future," in *Proc. of the American Control Conference*, St. Luis, 2009, pp. 2096-2103.
- [3] D. Wu, Z. Wang, "The Study of Multimode Power Control System for MW Variable-Speed Wind Turbine," *WSEAS Transactions on Systems*, vol.7, no. 10, 2008, pp. 890-899.
- [4] A.D. Hansen, P., Sorensen, F. Lov, F. Blaabjerg, "Control of variable speed wind turbines with doubly-fed induction generators," *Wind Engineering*, vol. 28, 2004, pp. 411-443.
- [5] O. Barambones, J.M.G De Durana, P. Alkorta, J.A. Ramos, M. De La Sen, "Sliding mode control law for a variable speed wind turbine," *WSEAS Transactions on Systems and Control*, vol. 6, no. 2, 2011, pp. 44-53.
- [6] K. Ro, H. Choi, "Application of neural network controller for maximum power extraction of a grid-connected wind turbine system," *Electrical Engineering*, vol. 88, 2005, pp. 45-53.
- [7] M. Soliman, O.P. Malik, D.T. Westwick, "Multiple Model predictive Control for Wind Turbines With Doubly Fed Induction Generators," *IEEE Transactions on Sustainable Energy*, vol. 2, no. 3, 2011, pp. 215-225.
- [8] M. Mirzaei, N.K. Poulsen, H.H. Niemann, "Robust Model Predictive Control of a Wind Turbine," in *Proc. of the American Control Conference*, Montreal, 2012, pp. 4393-4398.
- [9] H. Camblong, "Digital robust control of a variable speed pitch regulated wind turbine for above rated wind speeds," *Control Engineering Practice*, vol. 16, no. 8, 2009, pp. 946-958.

- [10] S. A. Frost, M. J. Balas, A. D. Wright, "Direct Adaptive Control of a Utility-Scale Wind Turbine for Speed Regulation," *Int. Journal of Robust Nonlinear Control*, vol. 19, no. 1, 2009, pp. 59–71.
- [11] D. Arzaghi-Haris, "Adaptive PID Controller Based on Reinforcement Learning for Wind Turbine Control," in *Proc. of the 6th WSEAS Conference on Environment, Ecosystems and Development*, Algarve, 2008, pp.15-21.
- [12] Y.D. Song, B. Dhinakaran, X.Y. Bao, "Variable speed control of wind turbines using nonlinear and adaptive algorithms," *Journal of Wind Engineering and Industrial Aerodynamics*, vol. 85, 2000, pp. 293-308.
- [13] X. Zhang, D. Xu, Y. Liu, "Intelligent control for large-scale variable speed variable pitch wind turbines," *Journal of Control Theory and Applications*, vol. 3, 2004, pp. 305-311.
- [14] R. Belu, "Fuzzy Control of a Variable Speed Wind Turbine for Standalone Applications," *Proc. of the 2nd WSEAS International Conference on Manufacturing Engineering, Quality and Production Systems*, Constantza, 2010, pp. 153-159.
- [15] D. Schlipf, D. J. Schlipf, M. Kühn, "Nonlinear model predictive control of wind turbines using LIDAR," in *Proc. Of AWEA WindPower Conference*, Anaheim, 2011.
- [16] T. Burton, D. Sharpe, N. Jenkins, E. Bossanyi, *Wind Energy Handbook*. Chichester: John Wiley And Sons Ltd, 2001.
- [17] J.D. Grunnet, M. Soltani, T. Knudsen, M. Kragelund, T. Bak, "Aeolus Toolbox for Dynamic Wind Farm Model, Simulation and Control," in *Proc. of the 2010 European Wind Energy Conference*, Warsaw, 2010
- [18] S. Thomsen, "Nonlinear Control of a wind turbine," M.S. thesis, Department of Informatics and Mathematical Modelling, Lyngby, Technical University of Denmark, Denmark, 2006.
- [19] J. Højstrup, "Velocity spectra in the unstable planetary layer," *Journal of the Atmospheric Sciences*, vol. 39, no. 10, 1982, pp. 2239–2248.
- [20] U. Maeder, M. Morari, "Offset-free reference tracking with model predictive control," *Automatica*, vol. 46, no. 9, 2010, pp. 1469-1476.
- [21] D. Simon, *Optimal State Estimation: Kalman, H-Infinity, and Nonlinear Approaches*, 2006, Wiley-Interscience.
- [22] J. Maciejowski, *Predictive Control with Constraints*. Englewood Cliffs, NJ: Prentice-Hall, 2000.
- [23] J. Novak, P. Chalupa, V. Bobal, "Multiple model modeling and predictive control of pH neutralization process," *International Journal of Mathematical models and Methods in Applied Sciences*, vol. 5, no. 7, 2011, pp. 1170-1179.
- [24] J.M. Jonkman, S. Butterfield, W. Musial, G. Scott, "Definition of a 5-MW reference wind turbine for offshore system development," Technical report, NREL, 2009.
- [25] A. Gosk, "Model Predictive Control of a Wind Turbine," M.S. thesis, Department of Informatics and Mathematical Modelling, Lyngby, Technical University of Denmark, Denmark, 2011.

Jakub Novak was born in Zlín, Czech Republic in 1978. He is a Researcher at Faculty of Applied Informatics of Tomas Bata University in Zlín, Czech Republic. He graduated from Faculty of Technology of the same university with an MSc in Automation and Control Engineering in 2002 and he received a PhD in Technical Cybernetics from Faculty of Applied Informatics in 2007. He is a researcher at the CEBIA-Tech research center at Tomas Bata University in Zlin. His research interests are modeling and predictive control of the nonlinear systems.

Petr Chalupa graduated in 1999 from Brno University of Technology and received the Ph.D. degree in Technical cybernetics from Tomas Bata University in Zlin in 2003.

He is a researcher at the CEBIA-Tech research center at Tomas Bata University in Zlin. His professional interests are adaptive and predictive control of real-time systems.